Relaying Strategies and Asymptotic Analysis for Half-Duplex Buffer-Aided Serial Relaying Systems

Sawsan El-Zahr and Chadi Abou-Rjeily, *Senior Member IEEE*

***Abstract*—In this paper, we investigate the problem of buffer-aided relaying in multi-hop systems that comprise a source, destination and K relays equipped with buffers of size L. We propose three relaying strategies and compare their performances. The three strategies account for the channel and buffer states at every time slot. The first strategy considers only the state of the previous relay buffer, the second accounts for the next relay whereas the third scheme accounts for the previous and next relays' states. We evaluate the asymptotic performance of the three schemes and we derive closed-form expressions of the diversity order (DO) and average packet delay (APD) for all values of K and L. Results show the ability of the three schemes to achieve multiple levels of tradeoff between the performance metrics.**

***Index Terms*—Serial relaying, multi-hop, buffer, performance analysis, outage probability, queuing delay, diversity order.**

I. Introduction

User cooperation is a promising solution to increase the efficiency and reliability of wireless systems [1]. Equipping relays with buffers proved to increase the degrees of freedom of systems but at the expense of an increased delay [2]–[4].

Dual-hop buffer-aided (BA) cooperative networks with half-duplex (HD) relays were studied in [2]–[4] where the information is relayed through a single relay selected from a cluster of relays in the vicinity of the source and destination nodes. The scheme in [2] activates the strongest available link where a link is available if the buffer at the transmitting node is not empty and the buffer at the receiving node is not full. Unlike [2] that only examines whether the buffers are full or empty, the actual numbers of packets stored in the relays' buffers were included in the relay selection policies in [3], [4]. The rationale is to increase the departure and arrival rates at congested and underfilled buffers, respectively, resulting in improved performance levels at the expense of an additional signaling overhead.

BA multi-hop relaying was tackled in [5] for mm-wave communications, in [6] for free-space optical communications and in [7]–[11] for radio-frequency (RF) HD communications.The *max-link* relaying protocol was proposed and analyzed in [7]–[9] where the available link with the maximum path gain is activated as in [2]. The Markov chain (MC) analysis in [9] concluded that the *max-link* scheme achieves the full diversity order only with infinite-size buffers along with a delay that increases with the buffer size. The multi-hop scheme in [10] improved on the *max-link* scheme and achieved delays that are independent of the buffer size L for $L \geq 5$. This scheme assigned weights based on the buffers' lengths to the links and selected the available link with the largest weight. To enhance the transmission throughput of BA multi-hop networks, a link selection scheme based on integrating the *max-link* and network-coding approaches was proposed in [11].

In BA networks, an inherent tradeoff exists between the diversity order (DO) and average packet delay (APD) where the reliability can be compromised for reducing the delay. The BA multi-hop strategy in [10] achieves two extreme cases of this tradeoff. (i): An APD-prioritizing scheme that guarantees the smallest possible APD at the expense of no gains in the DO that remains unimproved compared to buffer-free networks. (ii): A DO-prioritizing scheme that focuses on achieving the full DO with no regard to the APD that increases rapidly with the number of relays. Novel BA solutions must cope with the exigency of 5G applications that manifest a broad range of reliability and latency requirements. This paper focuses on this goal by suggesting tunable relaying schemes that can achieve a broad range of tradeoff levels between DO and APD thus offering an improved flexibility for 5G networks. The proposed schemes differ by the weights they assign to the first, last and intermediate hops where these weights are optimized for meeting any target DO level with the minimal APD.

II. System Model

Consider a decode-and-forward HD serial relaying network comprising a source S, a destination D and K relays R_1,..., R_K. A packet is transmitted from S to D in $K+1$ hops through the relays R_1 to R_K. We denote S and D by R_0 and R_{K+1}, respectively. A Rayleigh block fading channel model is assumed and we denote by Ω_k the variance of the channel gain of the k-th link. At a target rate r_0, the outage probability along the k-th link between R_{k-1} and R_k is given by [10]:

$$p_k = 1 - e^{-\frac{2^{(K+1)r_0}-1}{\Omega_k \bar{\gamma}}}, \tag{1}$$

where $\bar{\gamma} = P/\sigma^2$ is the average transmit signal-to-noise ratio (SNR) where P is the fixed transmit power and σ^2 is the variance of the zero-mean additive white Gaussian noise.

We assume that the relays are equipped with buffers of size L and we denote by $l_k \in \{0,\ldots,L\}$ the number of packets stored in the buffer B_k at R_k. The unavailability probabilities $\{q_k\}_{k=1}^{K+1}$ are given by $q_k(l_1,\ldots,l_K) = p_k + (1-p_k)\zeta$ where:

$$\zeta = \begin{cases} \delta_{l_1=L} & , k=1; \\ \delta_{l_{k-1}=0} + \delta_{l_k=L} - \delta_{l_{k-1}=0}\delta_{l_k=L} & , 2 \leq k \leq K; \\ \delta_{l_K=0} & , k=K+1. \end{cases} \tag{2}$$

where $\delta_{\mathcal{S}}=1$ if the statement S is true while $\delta_{\mathcal{S}}=0$ otherwise. In fact, link R_{k-1}-R_k is available only if the three following conditions are satisfied. (i): The channel between R_{k-1} and R_k is not in outage (with probability $1-p_k$). (ii): The buffer B_{k-1} (if any) at the transmitting node is not empty. (iii): The buffer B_k (if any) at the receiving node is not full.

The authors are with the Department of Electrical and Computer Engineering of the Lebanese American University (LAU), Byblos, Lebanon. (e-mails: sawsan.elzahr@lau.edu and chadi.abourjeily@lau.edu.lb).

III. Generalities and Relaying Strategies

A. Markov Chain and Performance Metrics

The MC framework constitutes the appropriate mathematical tool for analyzing queues [9], [10]. The MC comprises the $(L+1)^K$ states $(l_1, l_2, \ldots, l_K) \in \{0, \ldots, L\}^K$. The MC formulation directly yields the outage probability (OP) [9]:

$$OP = \sum_{(l_1,\ldots,l_K)\in\{0,\ldots,L\}^K} \pi_{l_1,\ldots,l_K} \prod_{k=1}^{K+1} q_k(l_1, \ldots, l_K), \quad (3)$$

where $\pi_{l_1,\ldots,l_K}$ stands for the steady-state probability of being in the state $(l_1, \ldots, l_K)$ when the MC reaches equilibrium. Equation (3) allows for the derivation of the DO defined as the negative slope of $OP(\bar{\gamma})$ on a log-log scale as $\bar{\gamma} \to \infty$.

The queuing at the buffers incurs delays. Denoting by $\bar{L}$ the average queue length, the APD is given by [9]:

$$APD = \frac{K + OP + (K+1)\bar{L}}{1 - OP}. \quad (4)$$

B. Weight-Based BA Multi-hop Relaying

The considered relaying strategies are based on assigning a weight Δ_k to link k for $k = 1, \ldots, K+1$ and activating the link $\hat{k}$ (between $\mathrm{R}_{\hat{k}-1}$ and $\mathrm{R}_{\hat{k}}$) with the largest weight:

$$\hat{k} = \arg\max_{k\in\mathcal{L}_a} \{\Delta_k\}, \quad (5)$$

where $\mathcal{L}_a \subset \{1, \ldots, K+1\}$ denotes the set of available links. If more than one link share the highest weight, the link closer to D will be selected to reduce the packet delay. The weights $\{\Delta_k\}_{k=1}^{K+1}$ in (5) depend on the buffer lengths $\{l_k\}_{k=1}^{K}$.

C. Related Works

The work in [10] proposed a weight-based multi-hop relaying strategy applying (5). This scheme, referred to as scheme 1 in what follows, privileges the transmission from congested buffers by assigning the following values to the weights $\{\Delta_k\}_{k=1}^{K+1}$:

$$\Delta_k = \begin{cases} s, & k = 1; \\ l_{k-1}, & k = 2, \ldots, K+1. \end{cases}, \quad (6)$$

where the parameter s is the weight associated with link 1.

The work in [10] advised a recursive algorithm for deriving the transition probabilities between the $(L+1)^K$ states of the MC (refer to eq. (7) in [10]). Once the transition probabilities are derived, the steady-state probabilities used in (3) can be readily obtained by applying standard MC techniques.

D. Novel Relaying Protocols

The proposed schemes differ by their choices of the weights and they will be referred to as scheme 2 and scheme 3.

Scheme 2 privileges the reception at under-filled buffers by assigning the following weights:

$$\Delta_k = \begin{cases} -l_k, & k = 1, \ldots, K; \\ -d, & k = K+1. \end{cases}, \quad (7)$$

where d is a parameter associated with link $K+1$.

Scheme 3 is based on the buffer lengths l_{k-1} and l_k at the transmitting and receiving nodes, respectively, as follows:

$$\Delta_k = \begin{cases} \alpha - l_1, & k = 1; \\ l_{k-1} - l_k, & k = 2, \ldots, K; \\ l_K - \beta, & k = K+1. \end{cases}, \quad (8)$$

where α and β are parameters associated with the first and last hops, respectively. For a finite buffer size L, the parameters s, d and (α, β) in (6), (7) and (8) should not exceed L.

IV. Asymptotic Performance Analysis

Even though an analysis that holds across the entire SNR range is desirable, such analysis is highly challenging and might be out of reach for all values of K and L for the following reasons. (i): The MC comprises a total of $(L+1)^K$ states where this number gets prohibitively large for large values of K and/or L. (ii): The MC is highly connected where each state can be reached from up to $K+1$ neighboring states. Moreover, the added value of the low-to-average-SNR analysis as compared to simulations is questionable since the exact steady-state probabilities of the $(L+1)^K$ states might be cumbersome and, hence, not useful for shedding more light on the system performance. In this context, a high-SNR analysis is more tractable, useful and better tailored to relaying systems that reap the highest performance gains at high SNRs. In fact, the asymptotic analysis focuses on a subset of dominant states containing only $K+1$ states each connected to one neighboring state where the improbable transitions at high SNR are ignored. This approach significantly simplifies the derivations without sacrificing the accuracy at high SNR and, as such, it yields simple closed-form expressions of the DO and asymptotic APD which allow us to study the impact of the parameters s, d and (α, β) on the system performance.

A. Closed Subset

The asymptotic analysis is based on the following observation. For the three considered schemes, we observe and prove the existence of a set of $K+1$ states $\mathcal{S} \triangleq \{\mathbf{s}_i\}_{i=1}^{K+1} \subset \{0, \ldots, L\}^K$ such that the transitions $\mathbf{s}_1 \to \mathbf{s}_2$, $\mathbf{s}_2 \to \mathbf{s}_3$, $\cdots$, $\mathbf{s}_K \to \mathbf{s}_{K+1}$ and $\mathbf{s}_{K+1} \to \mathbf{s}_1$ occur with a probability that tends to one asymptotically. The implications of the this observation are as follows. (i): At high SNR, the MC will be confined in the subset $\mathcal{S}$ where the probability of exiting this subset tends to zero asymptotically. As such, instead of deriving the steady-state probabilities for all $(L+1)^K$ states of the MC, it is sufficient to derive these probabilities only for the $K+1$ elements of $\mathcal{S}$. (ii): Since elements of $\mathcal{S}$ are connected to each other in a loop-like structure, then the asymptotic steady-state probability of each element of $\mathcal{S}$ is equal to $\frac{1}{K+1}$.

We denote by $\mathbf{s}_i(k) \in \{0, \ldots, L\}$ the k-th element of $\mathbf{s}_i$ which stands for the number of packets stored in B_k at steady-state. The ordered sequences of states of the closed subset $\mathcal{S}$ for schemes 1 and 2 are presented in (9) and (10), respectively:

$$\mathbf{s}_i(k) = \begin{cases} s - 1 + \delta_{k=i} & 1 \le i \le K; \\ s - 1 & i = K+1. \end{cases}, \quad (9)$$

TABLE I
CLOSED SUBSET OF SCHEME 3 FOR $\gamma > 0$

$\mathbf{s}_i(k)$	$1 \le k < \gamma$	$k = \gamma$	$\gamma < k \le K$
$i = 1$	$\alpha - k$	$\alpha - \gamma$	$\alpha - \gamma$
$1 < i \le \gamma$	$\alpha - k - \delta_{k=\gamma-i+1}$	$\alpha - \gamma + 1$	$\alpha - \gamma$
$i = \gamma + 1$	$\alpha - k$	$\alpha - \gamma + 1$	$\alpha - \gamma$
$\gamma + 1 < i \le K + 1$	$\alpha - k$	$\alpha - \gamma$	$\alpha - \gamma + \delta_{k=i-1}$

TABLE II
CLOSED SUBSET OF SCHEME 3 FOR $\gamma < 0$

$\mathbf{s}_i(k)$	$1 \le k \le K - \lvert\gamma\rvert$	$k = K - \lvert\gamma\rvert + 1$	$K - \lvert\gamma\rvert + 1 < k \le K$
$1 \le i \le K - \lvert\gamma\rvert$	$\alpha - \delta_{k=K-\lvert\gamma\rvert-i+1}$	$\alpha + 1$	$\alpha + \lvert\gamma\rvert - (K - k + 1)$
$K - \lvert\gamma\rvert < i < K + 1$	α	$\alpha + \delta_{k=i}$	$\alpha + \lvert\gamma\rvert - (K - k + 1) + \delta_{k=i}$
$i = K + 1$	α	α	$\alpha + \lvert\gamma\rvert - (K - k + 1)$

$$\mathbf{s}_i(k) = \begin{cases} d - \delta_{k=K-i+1} & 1 \le i \le K; \\ d & i = K+1. \end{cases} . \quad (10)$$

Define $\mathbf{s} \triangleq [\mathbf{s}_1^T \cdots \mathbf{s}_K^T]^T$ as the $K \times K$ matrix obtained by stacking the states $\{\mathbf{s}_i\}_{i=1}^K$ vertically. From (9), $\mathbf{s}_{K+1} = (s-1, \ldots, s-1)$ while $\mathbf{s} = (s-1)\mathbf{1}_K + \mathbf{I}_K$ where $\mathbf{1}_K$ is the $K \times K$ matrix whose elements are all equal to 1 and $\mathbf{I}_K$ is the identity matrix. From (10), $\mathbf{s}_{K+1} = (d, \ldots, d)$ and $\mathbf{s} = d\mathbf{1}_K - \mathbf{I}_K^{'}$ where $\mathbf{I}_K^{'}$ is the anti-diagonal matrix whose nonzero elements are equal to 1.

For scheme 3, the closed subset depends on the parameter $\gamma \triangleq \alpha - \beta$. For $\gamma = 0$, elements of $\mathcal{S}$ are provided in (11). For $\gamma > 0$ and $\gamma < 0$, the values of $\mathbf{s}_i(k)$ are reported in Table I and Table II, respectively.

$$\mathbf{s}_i(k) = \begin{cases} \alpha - \delta_{k=K-i+1} & 1 \le i \le K; \\ \alpha & i = K+1. \end{cases} . \quad (11)$$

In Appendix A, we prove that the transition $\mathbf{s}_i \to \mathbf{s}_{i+1}$ occurs with probability 1 for scheme 1 with $1 \le i \le K-1$. Similar proofs hold for all schemes and for all values of $i \in \{1, \ldots, K+1\}$ thus justifying the results in (9)-(11) and Tables I-II. These proofs are omitted for the sake of brevity.

B. DO and Asymptotic APD

Limiting the analysis to elements of $\mathcal{S}$ that are the most probable states in the MC, the asymptotic OP can be written as: $OP = \frac{1}{K+1} \sum_{i=1}^{K+1} \prod_{k=1}^{K+1} q_k(\mathbf{s}_i)$ following from (3). Since the unavailability probability q_k can be equal either to p_k or 1, then the DO can be determined from:

$$DO = \min_{i=1,\ldots,K+1} \{ \sum_{k=1}^{K+1} \delta_{q_k(\mathbf{s}_i)=p_k} \}, \quad (12)$$

since (1) behaves asymptotically as $\bar{\gamma}^{-1}$. The DO constitutes an important metric for capturing the performance of the fading-mitigation relaying techniques that achieve the highest performance gains at high SNRs [2]–[4], [7]–[10].

Since the asymptotic OP is several orders of magnitude smaller than K and L, then (4) can be approximated by $APD = K + (K+1)\bar{L}$ with $\bar{L} = \frac{1}{K+1} \sum_{i=1}^{K+1} \sum_{k=1}^{K} \mathbf{s}_i(k)$.

Therefore, the asymptotic APD and DO of the three proposed schemes are as follows.

For scheme 1 denoted by $Sc^{(1)}(s)$:

$$APD^{(1)}(s) = 2K + (s-1)K(K+1), \quad (13)$$

$$DO^{(1)}(s) = \begin{cases} 1, & s = 1; \\ K+1, & 1 < s < L; \\ K, & s = L. \end{cases} . \quad (14)$$

For scheme 2 denoted by $Sc^{(2)}(d)$:

$$APD^{(2)}(d) = dK(K+1), \quad (15)$$

$$DO^{(2)}(d) = \begin{cases} 1, & d = L; \\ K, & d = 1; \\ K+1, & 1 < d < L. \end{cases} . \quad (16)$$

For scheme 3, denoted by $Sc^{(3)}(\alpha, \beta)$, the asymptotic APD is given by:

$$APD^{(3)}(\alpha, \beta) = \begin{cases} \alpha K(K+1) & , \gamma = 0; \\ 2K + \beta K(K+1) + & \\ (\gamma - 1)\left(\frac{K+1}{2}\gamma - 1\right) & , \gamma > 0; \\ \alpha K(K+1) + \frac{\gamma^2 - \gamma}{2} + & \\ K\left(\frac{\gamma^2 + \gamma + 2}{2}\right) & , \gamma < 0. \end{cases} . \quad (17)$$

The DO depends on whether $\gamma = 0$, $\gamma > 0$ or $\gamma < 0$:

$$DO^{(3)}(\alpha, \beta) = \begin{cases} K, & \alpha = 1; \\ K+1, & 1 < \alpha < L; \\ 1, & \alpha = L. \end{cases} ; \ \gamma = 0, \quad (18)$$

$$DO^{(3)}(\alpha, \beta) = \begin{cases} K, & (\alpha, \gamma) = (L, 1); \\ K+1, & \alpha > \gamma; \\ \gamma, & \alpha = \gamma; \end{cases} ; \ \gamma > 0, \quad (19)$$

$$DO^{(3)}(\alpha, \beta) = \begin{cases} K, & \alpha \in \{1, L+\gamma\}; \\ K+1, & \text{elsewhere}; \end{cases} ; \ \gamma < 0. \quad (20)$$

The asymptotic APD expressions in (13), (15) and (17) follow directly from (9)-(11) and Tables I-II. In Appendix B, we provide highlights on how the DO of scheme 2 in (16) can be derived. Similar derivations hold for the two remaining schemes and are not provided here for conciseness.

C. Conclusions about the design of the BA relaying schemes

For scheme 3, (18) and (20) show that the diversity orders of K and $K+1$ can be achieved by $\gamma = 0$ and $\gamma < 0$. However, from (17), it can be observed that for the same value of α the APD is always smaller in the former case since $\frac{\gamma^2-\gamma}{2} > 0$ and $\frac{\gamma^2+\gamma+2}{2} > 0$ when γ is a nonzero negative integer. Therefore, the choice $\gamma < 0$ presents no advantage compared to the choice $\gamma = 0$ and the former option can be omitted.

The proposed schemes are capable of achieving different levels of tradeoff between DO and APD as highlighted below.

1) $DO = 1$: (14) and (19) show that $Sc^{(1)}(1)$ and $Sc^{(3)}(1,0)$ are capable of achieving this DO with an APD value of $2K$ following from (13) and (17). Similarly, (16) and (18) show that $Sc^{(2)}(L)$ and $Sc^{(3)}(L,L)$ can achieve $DO = 1$ but with an increased APD of $LK(K+1)$.

Therefore, $Sc^{(1)}(1)$ and $Sc^{(3)}(1,0)$ are the best delay-prioritizing schemes that achieve the smallest possible delay of $2K$ at the expense of a reduced $DO = 1$.

2) $DO = K+1$: $Sc^{(1)}(2)$, $Sc^{(2)}(2)$, $Sc^{(3)}(2,2)$ and $Sc^{(3)}(2,1)$ are all capable of achieving this maximum DO where the corresponding delays are K^2+3K, $2K^2+2K$, $2K^2+2K$ and K^2+3K, respectively. Note that, from (19), other values of α and γ (with $\alpha > \gamma$) can result in $DO = K+1$ when $\gamma > 0$. However, the choice $\alpha = 2$ and $\gamma = 1$ (implying that $\beta = 1$) is the best option since the APD in (17) increases with α and γ when $\gamma > 0$.

Therefore, $Sc^{(1)}(2)$ and $Sc^{(3)}(2,1)$ are the best outage-prioritizing schemes that achieve the highest possible DO of $K+1$ with an APD value of K^2+3K.

3) $DO = K$: This DO can be achieved by $Sc^{(1)}(L)$, $Sc^{(2)}(1)$, $Sc^{(3)}(1,1)$ and $Sc^{(3)}(L,L-1)$ with the smallest delay of $APD = K^2+K$ achieved by $Sc^{(2)}(1)$ and $Sc^{(3)}(1,1)$.

4) $DO \in \{2,\ldots,K-1\}$: (19) shows that only scheme 3 with $\gamma > 0$ can achieve such diversity orders when $\alpha = \gamma = DO$. Therefore, $Sc^{(3)}(DO,0)$ must be applied with $DO < K$. The corresponding APD is $2K + (DO-1)(\frac{K+1}{2}DO - 1)$ that increases with DO. Note that this delay must not exceed K^2+K since, otherwise, $Sc^{(2)}(1)$ and $Sc^{(3)}(1,1)$ will be better options since they achieve a smaller delay while increasing the DO to K. Therefore, $Sc^{(3)}(DO,0)$ is particularly appealing with large values of K where the achievable APD that increases linearly with K will fall below K^2+K.

Based on the above discussion and on the observation that scheme 1 and scheme 2 are easier to implement compared to scheme 3 (since the weights assume simpler expressions), the following conclusions can be drawn. (i): Scheme 1 is a good option capable of covering the extreme cases $(DO, APD) = (1, 2K)$ and $(DO, APD) = (K+1, K^2+3K)$ giving the full priority to the APD and DO, respectively. (ii): Scheme 2 is a suitable choice for achieving $(DO, APD) = (K, K^2+K)$ where, compared to the full-diversity case, DO is reduced by 1 with the advantage of reducing the APD by $2K$. (iii): Scheme 3 demonstrates the highest flexibility and can achieve all levels of tradeoffs between DO and APD.

V. Numerical Results

We fix $r_0 = 1$ and we let $\mathbf{\Omega} \triangleq [\Omega_1,\ldots,\Omega_{K+1}]$. Fig. 1 plots the APD as a function of K for $L = 5$, $\bar{\gamma} = 30$ dB and $\mathbf{\Omega} = [3,\ldots,3]$. Results show that the APD values in (13), (15) and (17) match the simulation results thus demonstrating the accuracy of the closed-form asymptotic expressions. Fig. 1 shows that the proposed schemes can achieve a wide range of tradeoffs between DO and APD for any number of relays. Compared with $Sc^{(2)}(1)$, $Sc^{(3)}(3,0)$ compromises the DO for the sake of achieving reduced APD values for $K \geq 5$. For $K = 5$, the former scheme is better since it achieves a larger DO and a smaller APD. Fig. 1 highlights on the increased delays of the *max-link* scheme in [9] where these delays significantly exceed those achieved by all three proposed schemes. While the *max-link* scheme achieves full diversity only with infinite-size buffers, the proposed schemes can achieve such diversity order with practical finite-size buffers. Moreover, the implementations of the proposed schemes are simpler compared to *max-link* since the exact values of the path gains are not included in the relay selection process.

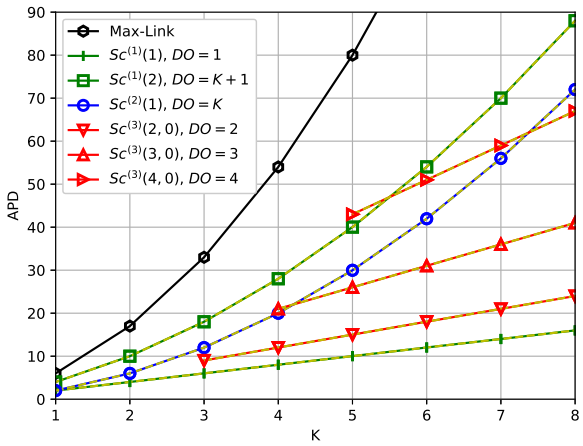

Fig. 1. APD for different scenarios with L=5. Solid lines and dashed lines represent the analytical and simulation values, respectively.

Fig. 2 and Fig. 3 show the OP and APD, respectively, for $K = 5$, $L = 5$ and $\mathbf{\Omega} = [2,3,2.5,2,3,3.5]$. Results highlight the close match between the theoretical and numerical results thus demonstrating the accuracy of the presented performance analysis. Results show the adjustability of the proposed schemes and on the impact of the control parameters s, d and (α,β) on the OP-APD tradeoffs. At $DO = 1$, $Sc^{(1)}(1)$ and $Sc^{(3)}(1,0)$ manifest exactly the same OP and APD performances. At $DO = K+1$, $Sc^{(1)}(2)$ achieves smaller OP levels compared with $Sc^{(3)}(2,1)$ at the expense of higher APD levels for small-to-average values of the SNR. At large SNRs, both schemes achieve the same asymptotic APD value of 40 as demonstrated in Section IV-C. At $DO = K$, $Sc^{(2)}(1)$ and $Sc^{(3)}(1,1)$ manifest comparable performances with a slight OP advantage and APD disadvantage of the former scheme. Finally, all eight variants of the proposed schemes in Fig. 2 and Fig. 3 result in significant APD reductions compared to [9].

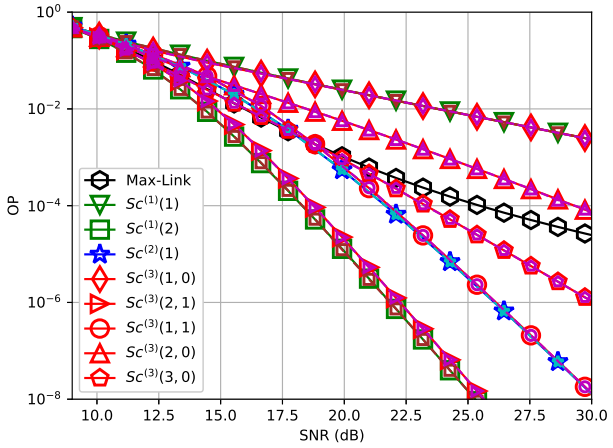

Fig. 2. OP for K=5 and L=5. Solid and dashed lines correspond to the theoretical and numerical results, respectively.

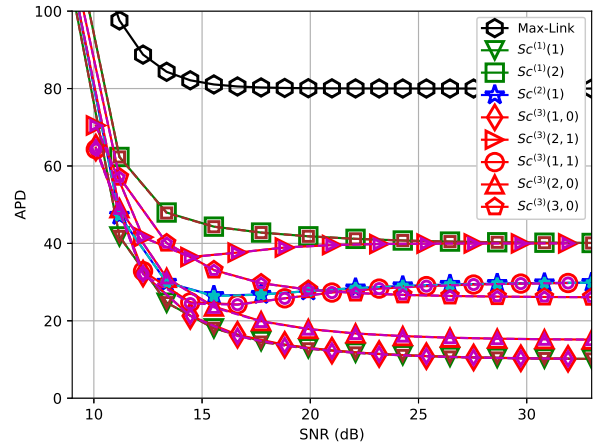

Fig. 3. APD for K=5 and L=5. Solid and dashed lines correspond to the theoretical and numerical results, respectively.

VI. Conclusion

We advised novel BA relaying schemes for HD multi-hop systems with an arbitrary number of relays. Based on a MC analysis and closed subset formulation, we identified the most probable states to derive closed-form expressions of the OP and APD. These expressions were essential for optimizing the control parameters of the tunable relaying schemes allowing to achieve different levels of tradeoff between outage and delay.

Appendix A

Consider an integer $i \in \{1, \dots, K-1\}$. From (9):

$$\mathbf{s}_i = (\underbrace{s-1, \dots, s-1}_{i-1 \text{ times}}, s, \underbrace{s-1, \dots, s-1}_{K-i \text{ times}}), \qquad (21)$$

implying from (6) that $\Delta_k = s$ for $k = 1, i+1$ and $\Delta_k = s-1$ otherwise. As such, link $i+1$ will be activated according to the tie-breaking rule. This implies that the number of packets in B_i will decrease by one while the number of packets in B_{i+1} will increase by one reflecting the flow of a packet from R_i to R_{i+1} along link $i+1$ assuming that all links are not in outage in the asymptotic regime. Therefore, $\mathbf{s}_i(i) \to \mathbf{s}_i(i) - 1 = s - 1$ and $\mathbf{s}_i(i+1) \to \mathbf{s}_i(i+1) + 1 = s$. The new state has the structure of $\mathbf{s}_{i+1}$ following from (21) implying a transition of the MC from state $\mathbf{s}_i$ to state $\mathbf{s}_{i+1}$.

Appendix B

Full and empty buffers contribute to decreasing the DO since they reduce the number of available links. From (2) and (12), $\mathbf{s}_i(k) = L \Rightarrow q_k(\mathbf{s}_i) = 1$ and $\mathbf{s}_i(k) = 0 \Rightarrow q_{k+1}(\mathbf{s}_i) = 1$.

From (10), for $i = 1, \dots, K$, one element of $\mathbf{s}_i$ is equal to $d-1$ while the remaining $K-1$ elements are equal to d and all elements of $\mathbf{s}_{K+1}$ are equal to d. (i): For $1 < d < L$, none of the elements of $\{\mathbf{s}_i\}_{i=1}^K$ and $\mathbf{s}_{K+1}$ is equal to 0 or L. As such, assuming that $p_k \to 0$ asymptotically for all values of k, all links in the network are available and $DO = K+1$. (ii): For $d = 1$, each state in $\{\mathbf{s}_i\}_{i=1}^K$ has one zero element corresponding to a single empty buffer while none of the elements of $\mathbf{s}_{K+1}$ is equal to 0 or L. Consequently, for each state in $\{\mathbf{s}_i\}_{i=1}^K$, one link out of the $K+1$ links is unavailable resulting in $DO = K$. (iii): For $d = L$, all buffers are full except for the buffer at R_{K-i+1} that contains $L-1$ packets for $i = 1, \dots, K$ from (10). Therefore, for each state in $\{\mathbf{s}_i\}_{i=1}^K$, two links are available; namely, link R_K-D and R_{K-i}-R_{K-i+1} implying that the corresponding summation in (12) is equal to 2. For $\mathbf{s}_{K+1}$, all buffers are full and only link R_K-D is available implying that the corresponding summation in (12) is equal to 1. As a conclusion, $DO = \min\{1, 2\} = 1$.

References

[1] J. S. Banerjee, A. Chakraborty, and A. Chattopadhyay, "A decision model for selecting best reliable relay queue for cooperative relaying in cooperative cognitive radio networks: the extent analysis based fuzzy ahp solution," *Wireless Networks*, vol. 27, no. 4, pp. 2909–2930, 2021.

[2] I. Krikidis, T. Charalambous, and J. S. Thompson, "Buffer-aided relay selection for cooperative diversity systems without delay constraints," *IEEE Trans. Wireless Commun.*, vol. 11, no. 5, pp. 1957–1967, May 2012.

[3] S. Luo and K. C. Teh, "Buffer state based relay selection for buffer-aided cooperative relaying systems," *IEEE Trans. Wireless Commun.*, vol. 14, no. 10, pp. 5430–5439, Oct. 2015.

[4] S. El-Zahr and C. Abou-Rjeily, "Threshold based relay selection for buffer-aided cooperative relaying systems," *IEEE Trans. Wireless Commun.*, vol. 2, no. 9, pp. 6210–6223, Sep. 2021.

[5] G. Yang, M. Haenggi, and M. Xiao, "Traffic allocation for low-latency multi-hop networks with buffers," *IEEE Trans. Commun.*, vol. 66, no. 9, pp. 3999–4013, May 2018.

[6] C. Abou-Rjeily and W. Fawaz, "Buffer-aided serial relaying for FSO communications: asymptotic analysis and impact of relay placement," *IEEE Trans. Wireless Commun.*, vol. 17, no. 12, pp. 8299–8313, Dec. 2018.

[7] L.-L. Yang, C. Dong, and L. Hanzo, "Multihop diversity - a precious source of fading mitigation in multihop wireless networks," in *IEEE Global Telecommun. Conf. (GLOBECOM 2011)*, 2011, pp. 1–5.

[8] C. Dong, L.-L. Yang, and L. Hanzo, "Performance analysis of multihop-diversity-aided multihop links," *IEEE Trans. Veh. Technol.*, vol. 61, no. 6, pp. 2504–2516, July 2012.

[9] B. Manoj, R. K. Mallik, and M. R. Bhatnagar, "Buffer-aided multi-hop DF cooperative networks: A state-clustering based approach," *IEEE Trans. Commun.*, vol. 64, no. 12, pp. 4997–5010, 2016.

[10] S. El-Zahr and C. Abou-Rjeily, "Buffer state based relay selection for half-duplex buffer-aided serial relaying systems," *IEEE Trans. Commun.*, accepted for publication.

[11] Z. Tian, Y. Gong, G. Chen, Z. Chen, and J. Chambers, "Buffer-aided link selection with network coding in multihop networks," *IEEE Trans. Veh. Technol.*, vol. 65, no. 9, pp. 7195–7206, Sep. 2015.